Science of the Total Environment 767 (2021) 144330

Contents lists available at ScienceDirect

Science of the Total Environment

journal homepage: www.elsevier.com/locate/scitotenv

Impact of COVID-19 lockdown upon the air quality and surface urban heat island intensity over the United Arab Emirates

Abduldaem S. Alqasemi [a,*], Mohamed E. Hereher [b,c], Gordana Kaplan [d], Ayad M. Fadhil Al-Quraishi [e], Hakim Saibi [f]

[a] Geography and Urban Sustainability, College of Humanities & Social Science, UAEU, Al-Ain, United Arab Emirates
[b] Geography Department, College of Arts and Social Sciences, Sultan Qaboos University, Muscat, Oman
[c] Environmental Sciences Dept., Faculty of Science, Damietta University, New Damietta, Egypt
[d] Institute of Earth and Space Sciences, Eskisehir Technical University, Eskisehir, Turkey
[e] Surveying and Geomatics Engineering Department, Faculty of Engineering, Tishk International University, Erbil, Kurdistan Region, Iraq
[f] Geology Department, College of Science, United Arab Emirates University, Al-Ain, United Arab Emirates

HIGHLIGHTS

- COVID-19 pandemic impact lockdown events in NEUAE greatly reduced the NO_2, AOD and SUHII concentrations.
- All Emirates in NEUAE showed decline in NO2, AOD and SUHII concentrations during lockdown period.
- The average NO2, AOD and SUHII concentrations were decreased by 23.7%, 3.7% and 19.2%, respectively.
- Validation for results showed a significant linear correlations between estimated and measured values.

GRAPHICAL ABSTRACT

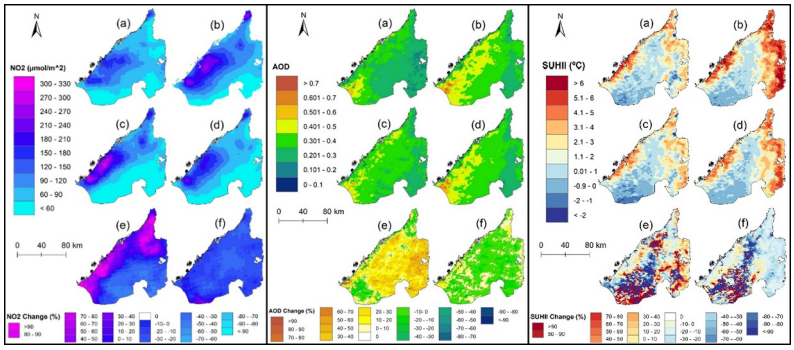

ARTICLE INFO

Article history:
Received 13 October 2020
Received in revised form 14 November 2020
Accepted 5 December 2020
Available online 25 December 2020

Editor: Prof. Pavlos Kassomenos

Keywords:
COVID-19
NO_2
AOD
SUHII
Lockdown
Northern emirates

ABSTRACT

The 2019 pandemic of Severe Acute Respiratory Syndrome-Corona Virus Diseases (COVID-19) has posed a substantial threat to public health and major global economic losses. The Northern Emirates of the United Arab Emirates (NEUAE) had imposed intense preventive lockdown measures. On the first of April 2020, a lockdown was implemented. It was assumed, due to lower emissions, that the air quality and Surface Urban Heat Island Intensity (SUHII) had been strengthened significantly. In this research, three parameters for Nitrogen Dioxide (NO_2), Aerosol Optical Depth (AOD), and SUHII variables were examined through the NEUAE. we evaluated the percentage of the change in these parameters as revealed by satellite data for 2 cycles in 2019 (March 1st to June 30th) and 2020 (March 1st to June 30th). The core results showed that during lockdown periods, the average of NO_2, AOD, and SUHII levels declined by 23.7%, 3.7%, and 19.2%, respectively, compared to the same period in 2019. Validation for results demonstrates a high agreement between the predicted and measured values. The agreement was as high as R^2=0.7, R^2=0.6, and R^2=0.68 for NO_2, AOD, and night LST, respectively, indicating significant positive linear correlations. The current study concludes that due to declining automobile and industrial emissions in the NEUAE, the lockdown initiatives substantially lowered NO_2, AOD, and SUHII. In addition, the aerosols did not alter significantly since they are often linked to the natural occurrence of dust

* Corresponding author.
E-mail address: a.alqasemi@uaeu.ac.ae (A.S. Alqasemi).

https://doi.org/10.1016/j.scitotenv.2020.144330

storms throughout this time of the year. The pandemic is likely to influence several policy decisions to introduce strategies to control air pollution and SUHII. Lockdown experiences may theoretically play a key role in the future as a possible solution for air pollution and SUHII abatement.

1. Introduction

The emergent Coronavirus disease 2019 (COVID-19) is a transmittable disorder characterized by severe acute respiratory syndrome coronavirus-2 (SARS-CoV-2) (Islam et al., 2020). By massive human-to-human transmission, COVID-19 has deeply hit the world and prompted a spike in the human mortality rate and massive economic casualties around the world (Bukhari and Jameel, 2020). The number of cases of Covid-19 globally hit approximately 34 million by the first of October 2020, while the number of deaths reached 1 million (WHO, 2020a). In late 2019, the first case of COVID-19 was identified in China and since then has spread very quickly throughout the world (Q. Li et al., 2020). On 11 March 2020, the World Health Organization (WHO) announced the novel coronavirus disease as a pandemic (WHO, 2020b). The WHO COVID-19 dashboard (https://covid19.who.int/) can be used to find the specifics of global COVID-19 cases. The first COVID-19 infection was reported in the United Arab Emirates (UAE) on 29 January 2020, and the first death was recorded on 21 March 2020. Since then, as per the Ministry of Health and Prevention (https://www.mohap.gov.ae/), there has been an alarming surge in active and death cases due to COVID-19.

In people with cardiovascular and respiratory disorders, the mortality risk of COVID-19 is substantially higher (Archer et al., 2020; Isaifan, 2020; Y. Zhu et al., 2020). Cardiovascular and respiratory disorders are also closely related to air pollution. Emissions leading to respiratory health conditions from primary pollutants containing particulate matter (aerosols) and gases such as nitrogen dioxide (NO_2) also have adverse environmental effects like soil and water acidification (Griffin et al., 2019; Mulenga and Siziya, 2019; Xu et al., 2020). The WHO (2020c) reports that approximately 4.2 million inhabitants die worldwide per year from factors primarily related to air pollution, which is currently increased, related to COVID-19 infected patients (Conticini et al., 2020; Wu et al., 2020). Also, recent worldwide studies on the effect of climate on the spread of the COVID-19 (Briz-Redón and Serrano-Aroca, 2020), showed that temperature and humidity are not crucial factors in the COVID-19 transmission, while precipitation, radiation, and wind speed have not been investigated in details.

Urban Heat Island (UHI) is among the most noticeable and frequently reported urbanization climatological consequences, by which urban and suburban regions are hotter than surrounding areas (rural/nonurban) (Hu and Brunsell, 2013; Miles and Esau, 2017). The negative influence of UHI is extensively described in the literature. For example, UHI causes rises in energy demand (Alghamdi and Moore, 2015), which implicitly leads to global climate change (Alghamdi and Moore, 2015), environmental degradation (Lin et al., 2017), air pollution (L. Zhu et al., 2020), impact to human comfort and health (Schwarz et al., 2011), and a degradation of ecosystem function (Keeratikasikorn and Bonafoni, 2018). All of these also play a significant role in the rise in the rate of COVID-19 cases (H. Li et al., 2020; Mukherjee and Debnath, 2020) and leads to heat-related deaths (Cui and De Foy, 2012; Lowe, 2016). UHI is measured based on air temperature, while satellite-derived Land Surface Temperature (LST) data is used to estimate the surface UHI (SUHI). Moreover, the calculation of SUHI Intensity (SUHII) requires observations from paired LST locations in both urban and rural/nonurban areas (Cui et al., 2019). LST is described as the surface temperature of the Earth's skin, playing an important role in the interchange of heat and energy among land surfaces and the atmosphere to assess changes in the environment (Moradi et al., 2018).

Distinct mitigation initiatives such as social distancing, cluster and whole lockdowns, comprehensive travel bans, mass quarantines, etc. have been introduced globally to mitigate the COVID-19 pandemic risk. Such risk mitigation initiatives have had a significant effect on socio-political ties and economic development at local and global levels (Ranjan et al., 2020a). Nevertheless, due to the reduction of anthropogenic-based pollutants, such precautionary strategies to prevent COVID-19 transmission have significantly enhanced air quality. The most critical challenge in the 21st century is the degradation of air quality worldwide due to the different sorts of anthropogenic interventions (Mehdipour and Memarianfard, 2017; Motesaddi et al., 2017). At such a moment, lockdown episodes enforced for the COVID-19 pandemic mitigation resulted in anti-environmental activities to cease as a byproduct. As a result, the level of air quality in the various continents of the Earth significantly improved since the COVID-19 pandemic began. Tobías et al. (2020) recorded a 45%, 51%, 31%, and 19% decline in the level of PM_{10}, NO_2, SO_2, and CO, respectively, over Barcelona in Spain within the lockdown span of a month. Isaifan (2020) recorded a substantial decrease in NO_2 and carbon emissions (30% and 25%, respectively) in China, which correlated to industrial lockdowns. Karuppasamy et al. (2020) documented a 55% contraction in NO_2 in India during the lockdown. A recent analysis in the Middle East has also shown a decrease in the number of air pollutants in Morocco of 75%, 49%, and 96% for PM_{10}, SO_2, and NO_2, respectively (Otmani et al., 2020). Moreover, in Iran, Nemati et al. (2020) recorded noticeable reductions in air pollution during the pandemic. Likewise, during the COVID-19 pandemic, many other recent studies show a significant decline in the level of air pollutants such as NO_2, SO_2, PM_{10}, $PM_{2.5}$, CO, etc. globally (Archer et al., 2020; Collivignarelli et al., 2020; Dantas et al., 2020; Islam et al., 2020; Kaplan and Avdan, 2020; Kerimray et al., 2020; Nakada and Urban, 2020; Ranjan et al., 2020a; Wang and Su, 2020). However, while studies generally showed a reduction in the primary pollutants, some studies showed no reduction in air pollution. For example, Q. Li et al. (2020), L. Li et al. (2020) and H. Li et al. (2020) investigated the air quality changes during the COVID-19 lockdown over 41 cities in the Yangtze River Delta Region. The results showed a decrease in some of the main pollutants, but still reported high $PM_{2.5}$ and increasing trend during the lockdown by over 20%. These contradictory results emphasize the need for continued detailed investigations on the topic.

The aforementioned studies concentrate primarily on evaluating the level of air pollutants during the pandemic scenario of COVID-19. Although a considerable correlation between air pollutants and LST was identified in some research (Alseroury, 2015; Feizizadeh and Blaschke, 2013; Hashim and Sultan, 2010; Kahya et al., 2016; Weng and Yang, 2006), the SUHII variability during the pandemic scenario has not yet been investigated. Like other nations, the UAE forced the shutdown of industries, public transit, airlines, vehicles, and other anthropogenic operations in all Emirates from the 1st April to the end of June 2020 to mitigate COVID-19 spread. Additionally, the UAE imposed a curfew daily between 8 pm and 6 am for residents (https://www.wam.ae). A full or partial lockdown is hypothesized to lead to improved air quality and reduce the SUHII since the lockdown is associated with many anthropogenic activities that directly impact the level of emissions. To our knowledge, no studies have examined the impacts of COVID-19 lockdowns on air quality and SUHII throughout the UAE. This current study was undertaken to investigate the potential impacts of COVID-19 lockdown operations on NO_2, Aerosol Optical Depth (AOD), and SUHII in the Northern Emirates of the UAE (NEUAE). This study also aims to validate satellite data over

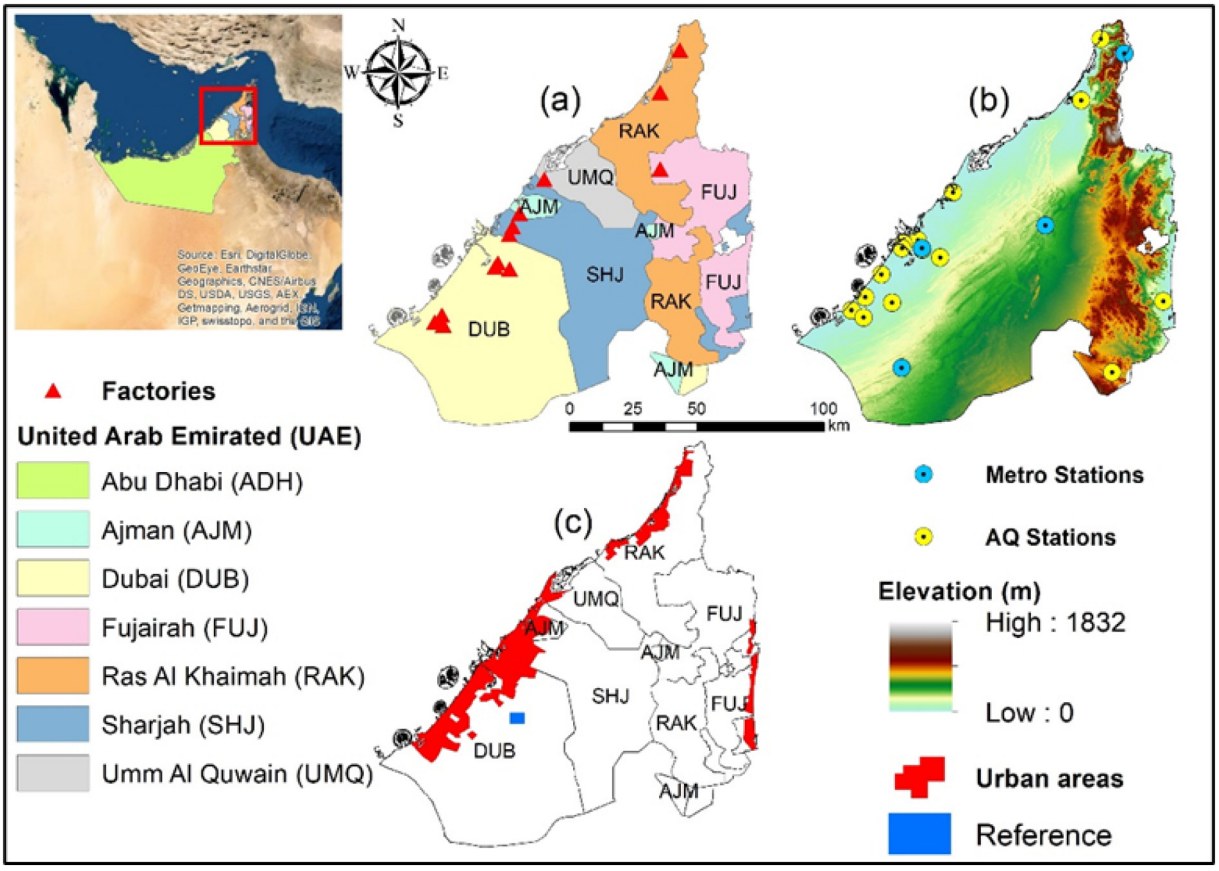

Fig. 1. Location map of the study area: (a) study area and major factories, (b) elevations and spatial distribution of meteorological and air quality stations, and (c) urban areas, and reference.

the study area using ground station records. Concentrating on the NEUAE, this work directly addresses the impact of lockdowns on air quality and SUHII, and is a resource for the science community and environmental protection policymakers, as well as resource in the development of an action plan to improve air quality and SUHII.

2. Data and methods

2.1. Study area

The United Arab Emirates (UAE) consists of seven federation Emirates (States): Abu Dhabi (ADH), and six northern Emirates, including Ras Al Khaymah (RAK), Dubai (DUB), Umm Al Qaywayn (UMQ), Sharjah (SHJ), Fujayrah (FUJ), and Ajman (AJM) (Fig. 1a). The Northern Emirates of the UAE (NEUAE) were chosen as a study area located approximately between latitudes 26° 365 to 26° 335 N and longitudes 54° 530 to 56° 240 E. Topography of the study area is mostly flat, with a mountain chain reaching an altitude of ~1800 m in the northeastern and eastern parts (Fig. 1b). The NEUAE is typically an arid region with a humid environment, located in the Arabian Peninsula's Eastern corner. It borders the Arabian Gulf to the north and the Gulf of Oman to the east (Fig. 1). The annual average air temperature is about 28 °C. It is much hotter (up to 45 °C) in the summer season (June to August) and colder (down to 10 °C) in the winter season (December to February) (https://www.ncm.ae/en/climate-reports-yearly.html?id=26). In the hot months, dust storms generally occur (Barbulescu and Nazzal, 2020). Over 80% of the yearly rainfall occurs in the winter season (FAO, 2008).

Around 71% of the UAE population is based in the NEUAE. Around 50% of the population resides in DUB, followed by 31% in SHJ, and only 1% resides in UMQ, as per the Federal Competitiveness and Statistics Authority (https://fcsa.gov.ae/ar-ae/Pages/home.aspx). Besides that, as documented by the United Nations (2019), more than 86.5% of the NEUAE people live in urban areas situated on the coastline (Fig. 1c). Furthermore, over the past two centuries, fast and pervasive economic and political change has caused increased population explosion, accelerated urbanization, higher energy consumption, and increased vehicular and industrial emissions (Alawadi et al., 2018). This all adds to a net increase in all anthropogenic activities.

2.2. Data

Between March to June 2019 and 2020, two different air pollutants NO_2 and AOD, and night LST data were collected for the NEUAE. The average monthly NO_2 and AOD data were acquired from Google Earth Engine (GEE). NO_2 is measured by the Sentinel-5p TROPOMI (Tropospheric Monitoring Instrument) mission of Copernicus ESA. While AOD and night LST were obtained by MODIS MAIAC (MCD19A2) and MODIS Aqua (MYD11A2), respectively. Due to the finite temporal scope of Sentinel-5p data, it is worth noting that the baseline was 2019. A summary of the datasets used in this study is shown in Table 1.

2.2.1. TROPOMI/Sentinel-5p data (NO_2)

TROPOMI was launched on 13th October 2017 as a passive hyperspectral nadir-viewing imager aboard the Sentinel-5 Precursor satellite, which is also recognized as Sentinel-5P (Veefkind et al., 2012). Sentinel-5P is a near-polar orbiting sun-synchronous satellite positioned at an altitude of 817 km in an ascending node with an equator crossing time at 13:30 (local time) offering daily worldwide coverage. Furthermore, since July 2018, TROPOMI delivered calibrated data from its nadir-viewing spectrometer that measures reflected sunlight in the ultraviolet, visible, near-infrared, and shortwave infrared with seven bands, where the fourth band spectral range is 405–500 nm, which could be used for NO_2 monitoring (Venter et al., 2020). Recent works have shown that measurements of TROPOMI are quite well

Table 1
Summary of the datasets used in this study.

Data source	Parameter	Spatial resolution	Temporal resolution	Data access link
Sentinel5p TROPOMI	NO_2	3.5 × 5 km	Daily	
MODIS MAIAC	AOD	1 × 1 km	Daily	https://lpdaac.usgs.gov/
MODIS/ AQUA	Night LST	1 × 1 km	8-day	https://lpdaac.usgs.gov/
SRTM	DEM	30 × 30 m	–	https://earthexplorer.usgs.gov/
NCM	NO_2 &$PM_{2.5}$	–	Monthly	–
DM	Ta_{min}	–	Monthly	–

associated with actual ground measures of NO_2 (Griffin et al., 2019; Lorente et al., 2019). TROPOMI products included in this research are L3 offline version products. Band four's spectral and spatial resolutions are 0.55 nm and 5.5 × 3.5 km, respectively, and the signal to noise ratio is also massively enhanced (Cheng et al., 2019).

2.2.2. MODIS data (AOD and LST)

In a near-polar solar-synchronous circular orbit, the Moderate Resolution Imaging Spectroradiometer (MODIS) was launched onboard NASA's Aqua and Terra satellites. Local crossing times are approximately 01:30 and 13:30 for the Aqua satellite and 10:30 and 22:30 for the Terra satellite. MODIS has a 2330 km (cross-track) swath and provides near-global coverage daily. MODIS is an imaging radiometer with 36 wavebands, covering the wavelength spectrum from the visible to the thermal infrared. AOD data was possessed from the cloud-masked MCD19A2-v6 product, which is a MODIS Terra and MODIS Aqua combined AOD retrieved with the Multi-Angle Implementation Atmospheric Correction (MAIAC) algorithm (Lyapustin et al., 2018). This dataset has previously been used effectively to map ground-level $PM_{2.5}$ concentrations (Wei et al., 2019). In this analysis, AOD at 550 nm (i.e., the green band) was utilized because of its superior accuracy as shown by previous studies (Lyapustin and Wang, 2018). Concerning night LST data, for 2019 and 2020, MODIS Aqua's MYD11A2-v6 performance entails an 8-day composite of LST data at night from 1 March to 30 June 2019 and 2020. In the long time series, the 8-day LST composite products will undervalue the quantity of gaps created by clouds or other unwanted circumstances, that are beneficial for SUHII studies to conduct a spatial comparison (Hu and Brunsell, 2013; Schwarz et al., 2011). Modern Time LST products (v6) have resolved past version accuracy issues. Additionally, measure errors and validation assessments in bare land and arid regions currently suggest their use in these areas (Lu et al., 2018). For the present work, MAIAC AOD and night LST data on a 1 km nadir resolution were retrieved from the NASA Land Processes Distributed Active Archive Center (Table 1).

2.2.3. SRTM data (DEM)

The SRTM DEM data was downloaded from the USGS Earth Explorer (Table 1) to pick a suitable reference location for SUHII calculation. The area's topography is predominantly flat but increases slowly from the northwest to southeast and east, reaching approximately 1830 m (Fig. 1b). The Digital Elevation Model (DEM) 30 m resolution was used for this study. The DEM model was obtained from the Shuttle Radar Topography Mission (SRTM).

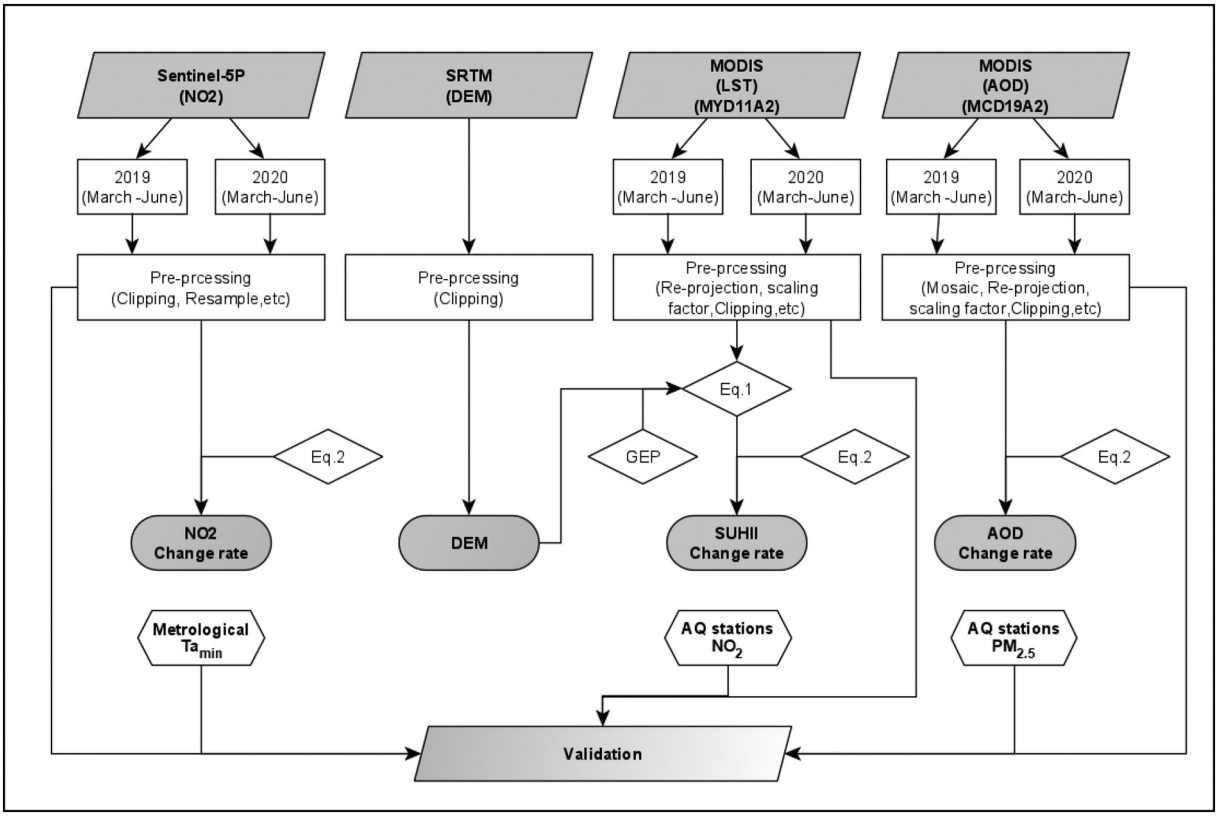

Fig. 2. Workflow flowchart adopted in the present study.

2.2.4. Meteorological data

The air quality and meteorological records utilized in our study were collected from the Municipality of Dubai (DM) and the National Center of Meteorology (NCM) for validation. From the aforementioned sources, three parameters were obtained: NO_2, $PM_{2.5}$, and minimum air temperature (Ta_{min}) for each of the years 2019 and 2020, from March to June. Ta_{min} was chosen for the highest degree of matching with MODIS night LST overpass time, which is closer to Ta_{min} (Alqasemi et al., 2020). Likewise, $PM_{2.5}$ was selected as AOD, which is considered a proxy for $PM_{2.5}$ (Fan et al., 2020; Venter et al., 2020).

2.3. Methods

2.3.1. Data pre-processing

Usually, the products MCD19A2 and MYD11A2 were available in the sinusoidal grid projection that was re-projected to the WGS 1984 geographic coordinate system. In addition, a mosaic of two tiles was created with MYD11A2 data. The scale factor was multiplied by both MCD19A2 and MYD11A2. Then, we subtracted 273.15 to produce a night LST in Celsius, from the reported Kelvin. In the process of producing a seamless dataset, every unrealistic LST data, values above 100 °C and/or below −50 °C, or any value outside the acceptable range was labeled as no data and ignored. Only reliable pixels and high-quality data were used as per the layer of Quality Assessment (QA). Missing values were amended using the mean value of each series. Afterward, night LST data was aggregated to a monthly period by averaging the 8-day composite data to obtain monthly average night LST. As for TROPOMI-Sentinel-5P, NO_2 was resampled to 1 × 1 km to ensure conformity with a spatial resolution of MODIS data (i.e., AOD and night LST). Finally, the boundary polygon that defined the study area was used to clip all datasets.

As a preventive strategy for COVID-19, the three months of April, May, and June (AMJ) were averaged as one period applied for all datasets throughout the NEUAE. The March month was collected and processed for pre-lockdown in 2020 for NO_2, AOD, and night LST. Similarly, for the identical time spans as the lockdown and pre-lockdown periods, the mean of datasets was obtained for 2019 for comparative analysis, as well as utilized for evaluating the correlation with measured data from ground stations.

2.3.2. SUHII calculation

The night SUHII is a distinctive feature of arid regions, as cited by previous researchers (Alahmad et al., 2020; Clinton and Gong, 2013; Lazzarini et al., 2013). Additionally, the lowest surface temperature is reported at midnight, making Aqua night data an optimal choice near the SUHII maxima. SUHII is typically measured from the LST contrasts between urban and surrounding areas (will be cited here as reference). Consequently, choosing a reliable reference is important. In different tests, however, the approaches for determining the reference differed extensively in various studies. The reference should not be influenced by urban, high altitude, vegetation, or water (Hu et al., 2019). Therefore,

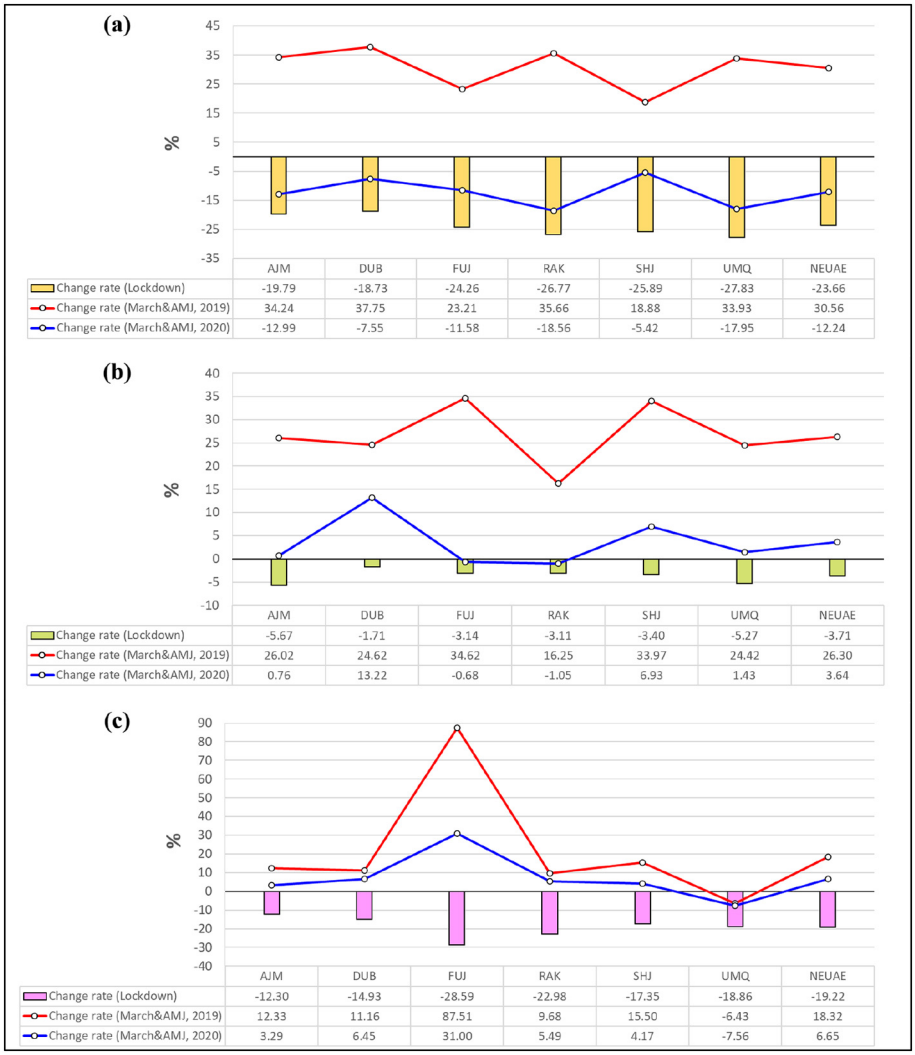

Fig. 3. Average concentrations of (a) NO_2, (b) AOD, and (c) SUHII in the NEUAE before and during the COVID-19 lockdown, compared to the same 2019 time period.

in this study, the reference was defined as bare land using chronological images from Google Earth Pro (GEP) with elevation lower than 50 m as determined by the 30 m DEM dataset, to prevent the cooling effect on the SUHII quantification. Finally, by subtracting the average night LST of the reference from the night LST of all pixels, the SUHII was calculated for every pixel utilizing the following equation (Eq. (1)):

$$SUHII = LST_{PX} - LST_{RF} \quad (1)$$

where LST_{PX} is the night LST of all pixels, and LST_{RF} is the mean night LST of the reference.

2.3.3. Change rate (concentration)

It is critical to understand the change in the NO_2, AOD, and SUHII concentrations throughout the lockdown period. After retrieving the data on pollutants and SUHII, the Spatiotemporal pattern of average levels of NO_2, AOD, and SUHII was categorized into four groups; (i) pre-lockdown (March 2020); (ii) during the lockdown period (AMJ, 2020); (iii) the same Pre-lockdown dates (March 2019); (iv) the same 2019 lockdown dates. Furthermore, the change rates were calculated utilizing Eq. (2) to reflect the percentage of change in the study area's NO_2, AOD, and SUHII levels during the lockdown period related to the past year (i.e., 2019) for the same period, which were also compared to pre-lockdown in March 2020. The change rate of variation between March and AMJ throughout 2019 and 2020 was also examined.

$$\text{Change rate } (\%) = ((X2020 - X2|019)/X2019)*100 \quad (2)$$

where, X is NO_2, AOD, or SUHII for the selected periods in 2019 and 2020. Also, the correlation was analyzed by calculating the regression coefficients (R^2) among stations and satellite data based on the availability of the metrological and air quality station data. The flowchart for the methodological workflow is presented concisely in Fig. 2. The sequence of data collection, pre-processing, clipping, resampling, data extractions, and SUHII measurement, change rate, and validation are described in Fig. 2. For the processing, analysis, and exhibition, the ESRI ArcGIS™ version 10.4 software framework and Microsoft Office Excel were used.

3. Results and discussion

3.1. Nitrogen dioxide (NO_2)

A dramatic drop in NO_2 concentration was recorded during the lockdown period (i.e., AMJ, 2020) in the NEUAE due to the COVID-19. Fig. 4

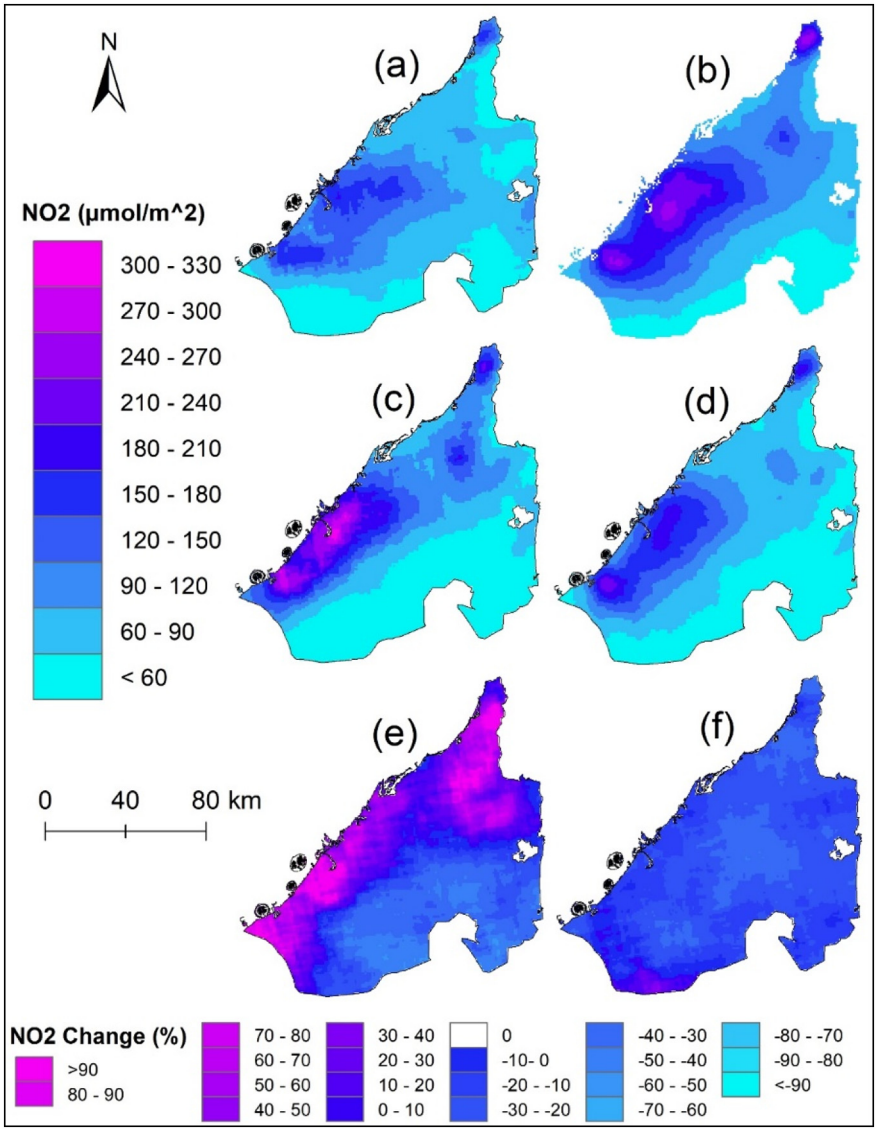

Fig. 4. Spatiotemporal distribution of average NO_2 over the NEUAE: (a) March 2019, (b) average AMJ 2019, (c) pre-Lockdown (March 2020), (d) during Lockdown (AMJ 2020), (e) percentage of change between March 2019 and 2020, and (f) percentage of change between average AMJ 2019 and 2020.

depicts the substantial spatiotemporal changes in NO_2 levels throughout lockdown and pre-lockdown in the NEUAE. The analysis showed that the six Emirates experienced a decline in NO_2 levels because of restricted transportation and factories' closure. This result is compatible with other earlier studies undertaken in various regions around the globe (Baldasano, 2020; Dantas et al., 2020; Islam et al., 2020; Kaplan and Avdan, 2020; Sharma et al., 2020). Fig. 3a indicates that RAK experienced the highest decline in NO_2 levels among the six Emirates (18.6%), followed by UMQ (~18%), AJM (13%), and FUJ (11.6%) compared with the average NO_2 levels throughout lockdown with the average levels immediately pre-lockdown, for other Emirates relative to DUB (7.6%) and SHJ (5.4%). In addition, our study indicates that, as shown in Fig. 3a, the average decline in NO_2 concentration throughout NEUAE was substantial 12.2%. This decline should be noted that NO_2 emission is closely connected to fuel combusting within the factories area (Figs. 1a & 4). Therefore, the limitations on these areas' operations are hypothesized to correlate to the substantial drop in NO_2 level throughout the lockdown period. Additionally, within March 2019, the NO_2 level was lower than March 2020, as shown in Fig. 3a and c, which may be due to higher precipitation during March 2019.

A substantial decrease in NO_2 is visible in the study area by comparing the NO_2 values during the 2020 lockdown period with the identical 2019 time period. The maximum calculated decline was for UMQ (27.8%) followed by RAK (26.8%), SHJ (~26%), FUJ (24.3%), AJM (19.8%) and DUB (18.7%). The average reduction was 23.7% with the whole study area (Fig. 3a). These results are in accordance with the results of previously published research. Islam et al. (2020) recorded identical outcomes for Bangladesh, Agarwal et al. (2020) recorded an average reduction in NO_2 during the lockdown in China by 49% and in Mumbai (India) by more than 76%. In the Middle East (Morocco), NO_2 levels were decreased during the lockdown phase as well (Sekmoudi et al., 2020). This decline in NO_2 concentrations shows that lockdown initiatives related to the COVID-19 pandemic significantly impacted NO_2 concentrations in the NEUAE as well as elsewhere.

3.2. Aerosol optical depth (AOD)

The average AOD values during the lockdown period were lower than the mean AOD values in 2019 for the equivalent time frame, as shown in Fig. 5. The analysis indicates that all six Emirates encountered

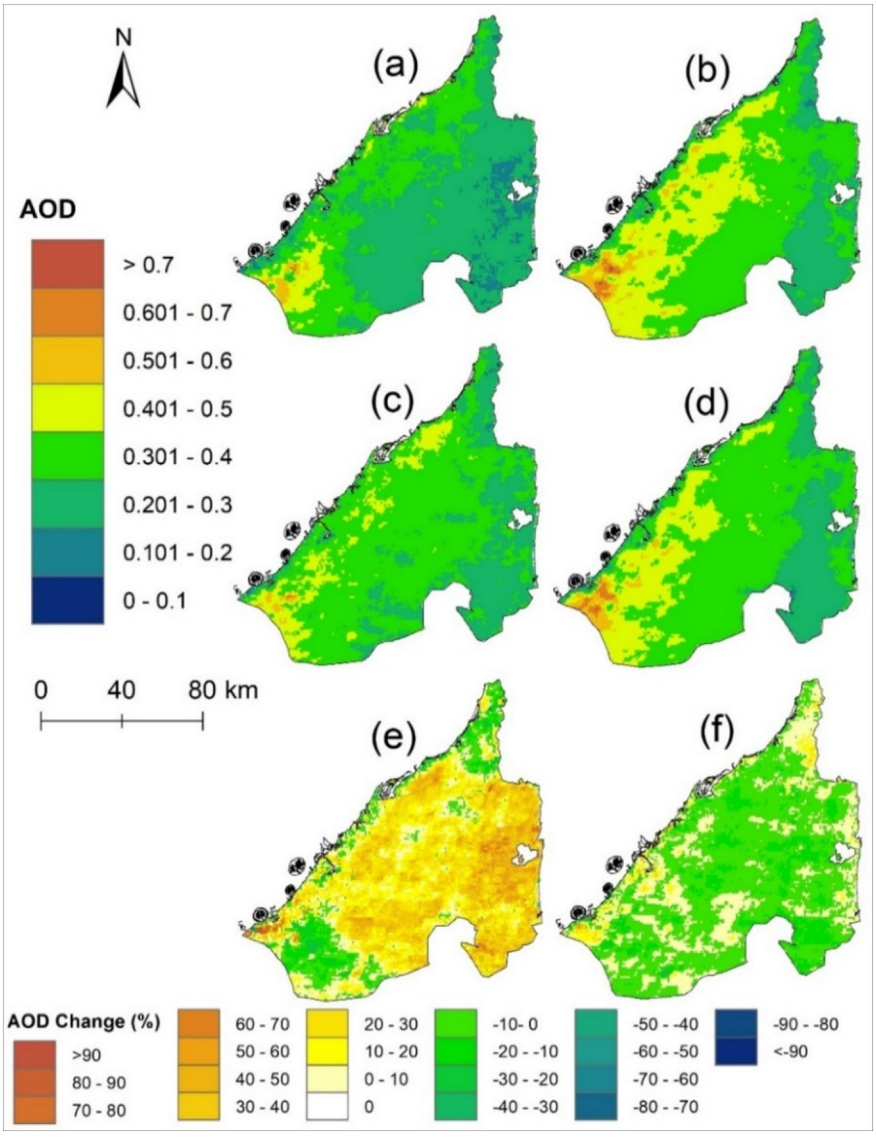

Fig. 5. Spatiotemporal distribution of average AOD over the NEUAE: (a) March 2019, (b) average AMJ 2019, (c) pre-lockdown (March 2020), (d) during lockdown (AMJ 2020), (e) percentage of change between March 2019 and 2020, and (f) percentage of change between average AMJ 2019 and 2020.

a decline in AOD concentration because of restricted aerosol sources, specifically, burning biomass, emissions from factories, vehicles, heavy transport, machinery (Ranjan et al., 2020b), and dust (Khuzestani et al., 2017). Therefore, a reduction in AOD due to the restrictions of industrial and automobile movement is reasonable. The spatiotemporal variations in AOD concentrations in the NEUAE (Fig. 5) show that AJM with 5.7% and UMQ with 5.3% were the largest declines, followed by SHJ with 3.4%, FUJ and RAK, both with 3.1%, and, in Dubai, the lowest drop, 1.7%. The rate of change was 3.7% throughout the overall study area (NEUAE), as shown in Fig. 3b. Similarly, a common declining trend of AOD has been recorded in China (Fan et al., 2020; Filonchyk et al., 2020), India (Gautam, 2020; Pathakoti et al., 2020; Ranjan et al., 2020b), and South Asia (Zhang et al., 2020).

During the average AMJ, the level of AOD increased significantly compared to March (Fig. 5). This may be due to the fact that rainfall throughout these months (AMJ) is scarce, and the gusty winds ensure that dust storms become frequent (Barbulescu and Nazzal, 2020; Karagulian et al., 2019). Furthermore, according to Al Otaibi et al. (2019), AOD typically rises over the gulf nations in hot summer months. Consequently, there is generally a rise in the AOD level in AMJ when compared to March. However, the change rate between March and the average AMJ in 2020 decreased relative to the past year for all six Emirates, as shown in Fig. 3b. In 2019, the change rate over the NEUAE was 26.3%, whereas it dropped in 2020 to 3.6%. Notably, AOD emission is linked with the major industries, particularly in Dubai (Figs. 1a, 5). Furthermore, Dubai recorded the smallest reduction in AOD. The most populous and established region of the UAE is the Emirate of Dubai, which includes the most industrialized regions. Therefore, certain additional considerations may explain the relatively small reduction in Dubai.

3.3. Surface Urban Heat Island Intensity (SUHII)

SUHII specifically portrays urbanized areas and mountains, as shown in Fig. 3(a–d). A drop in SUHII levels was also recorded, like NO_2 and AOD (Fig. 3f), also attributed to the partial or full nationwide lockdown. The result reveals that during the specific time frame, nighttime SUHII levels over this duration were comparatively less than the 2019 levels (Figs. 3c & 6). The decline was generally identified in all Emirates, varying from 12.3% to 28.6%, in which the average drop is 19.2% across the whole study area.

The maximum SUHII concentrations are found in FUJ (28.6%) and RAK (23%) as displayed in Fig. 3c, which may be due to the elevations

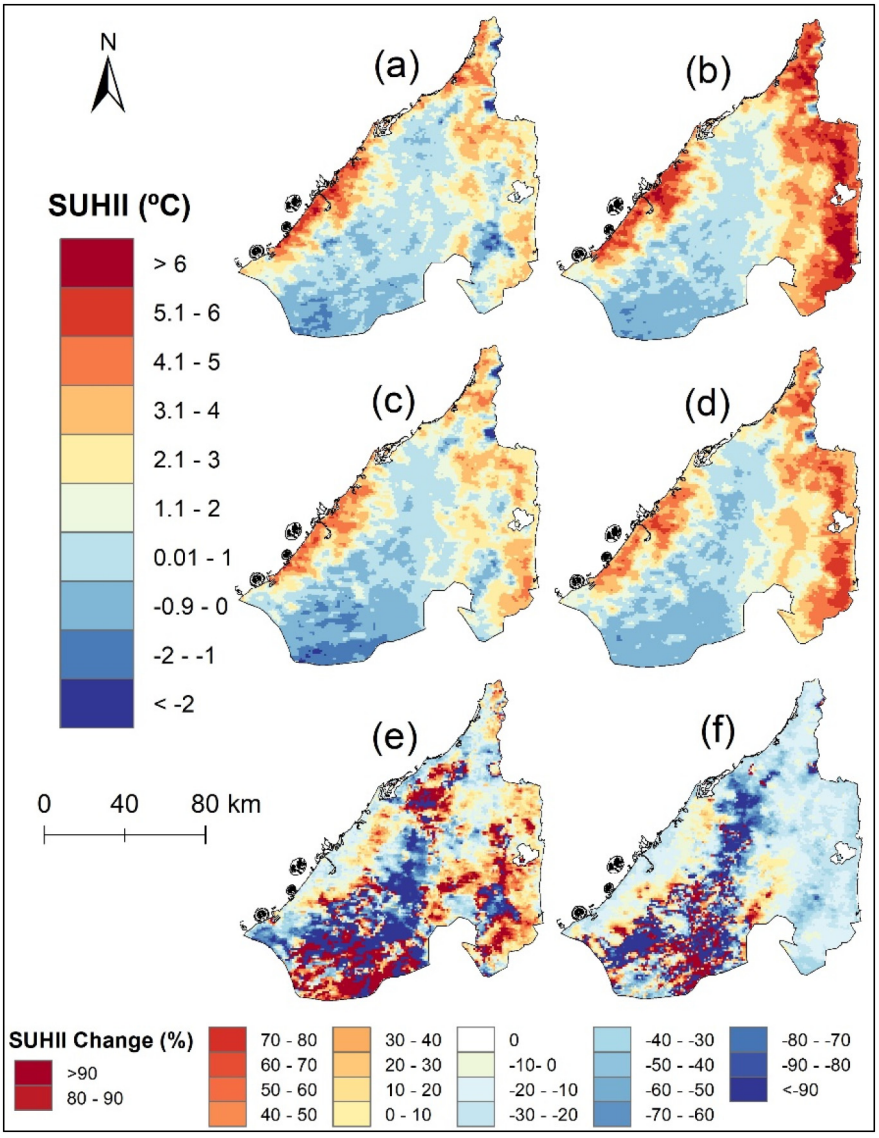

Fig. 6. Spatiotemporal distribution of SUHII over the NEUAE: (a) March 2019, (b) average AMJ 2019, (c) pre-Lockdown (March 2020), (d) during Lockdown (AMJ 2020), (e) percentage of change between March 2019 and 2020, and (f) percentage of change between average AMJ 2019 and 2020.

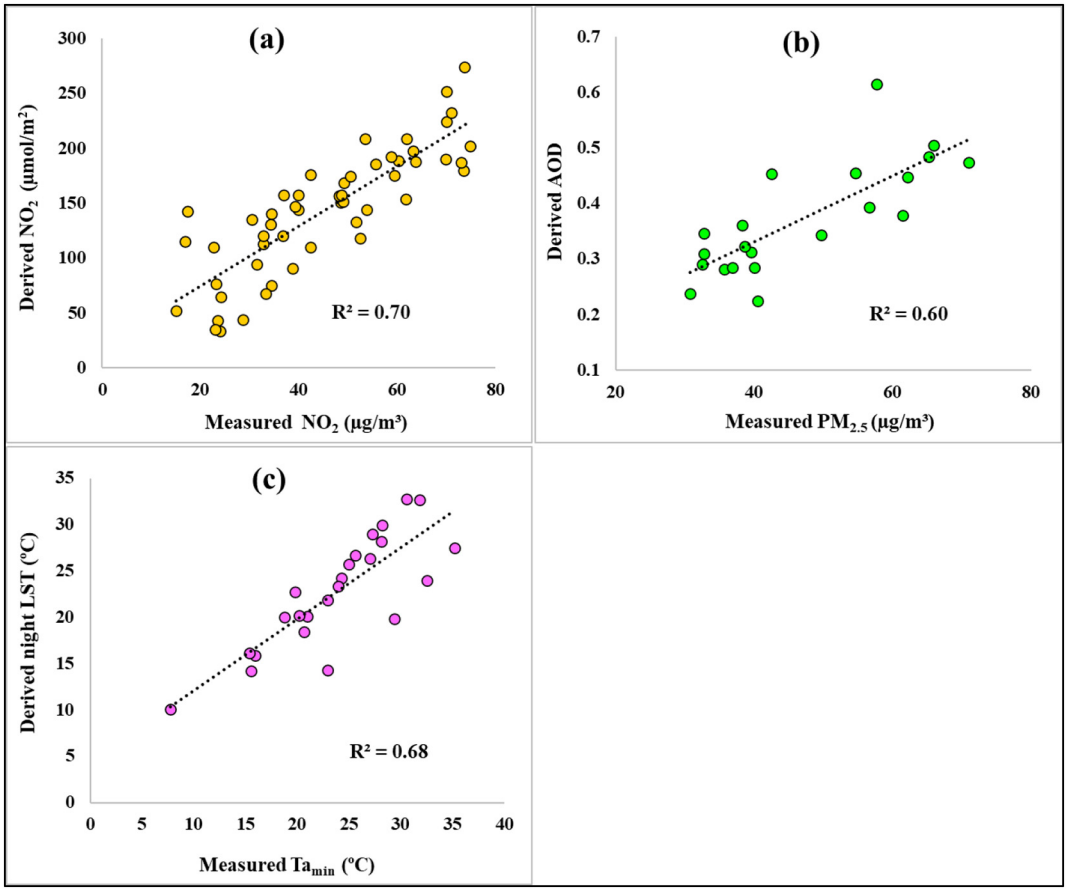

Fig. 7. The scatter plots for validation of the derived data from satellites and measured data from ground-measuring stations; (a) measured NO_2 and derived NO_2, (b) measured $PM_{2.5}$ and AOD, and (c) minimum air temperature (Ta_{min}) and night LST.

and type of rocks. Fig. 6(a–d) also reveals that SUHII increases during AMJ relative to March, related to heat emission in hot months (e.g., air conditioning system). Nevertheless, the change rate in 2020 between March and AMJ is less than in 2019. SUHII change rate dropped from 18.3% in 2019 to 6.7% in 2020 over the NEUAE, as exhibited in Fig. 3c. Overall, the results indicate a reduction in SUHII values as a result of the shutdown of anthropogenic activities and sources of heat emissions such as industrial processes, power plants, flight, and transport.

3.4. Validation

In this section, the validations of derived data from satellites with the measured data from actual ground stations are investigated. The comparisons between derived NO_2, AOD, and night LST plotted against the measured data NO_2, $PM_{2.5,}$ and minimum air temperature (Ta_{min}), respectively, are presented in Fig. 7. Based on the availability of ground station data, the validation of the NO_2 and $PM_{2.5}$ data were made using thirteen and five air quality monitoring stations measurements, respectively, from March to June 2019. Ta_{min} data covers the whole period (March–June) in 2019 and 2020 at four metrological stations (Fig. 1b). Night Aqua LST data is validated with Ta_{min} because the Aqua satellite crosses the equator at night, close to the Ta_{min}; therefore, this is the most appropriate temperature measurement for validation purposes. In addition, as mentioned before, the AOD is considered a proxy for ($PM_{2.5}$); thus, AOD is plotted versus $PM_{2.5}$.

Our comparisons show that the TROPOMI Sentinel-5P NO_2 is highly correlated with the air quality monitoring stations data with $R^2 = 0.70$, as shown in Fig. 7a. Likewise, Fig. 7(b) shows the scatter plot of measured $PM_{2.5}$ versus MODIS MAIAC AOD. The statistical analyses showed a high coefficient of determination ($R^2 = 0.60$). Similarly, a high correlation was found between the MODIS Aqua night LST and the Ta_{min} from station measurements ($R^2 = 0.68$), as displayed in Fig. 7c. Overall, a good agreement is found between satellite data and actual measured data; hence, the satellite observations are a valuable resource for studying air pollution and SUHII over large geographic regions.

4. Conclusions

The impact of anthropogenic activities lockdown due to the COVID-19 pandemic on air quality and SUHII in the NEUAE was studied by examining NO_2, AOD, and SUHII levels and evaluating variations in spatial distribution. To demonstrate how restrictive anthropogenic activities throughout the COVID-19 lockdown minimized the air pollutants and SUHII in NEUAE, satellite data of different parameters were used and compared between 2019 and 2020. As predicted, the current investigation discovered that NO_2, AOD, and SUHII concentrations across the NEUAE decreased during the pandemic lockdown. The largest average drop was in NO_2 (23.7%) followed by SUHII (19.2%) and AOD (3.7%) throughout the lockdown period compared with the same period in 2019.

This study showed that the satellite derived measurements of the selected air pollutants and SUHII data are highly correlated with the actual measured data. Therefore, satellite data is a significant and reliable resource for researching air quality and SUHII because of the spatial coverage and cost-effectiveness of the data, especially for developing countries like the UAE. We conclude that our study has established a benchmark paradigm that will potentially assist the authorities concerned with the potential management of air quality and SUHII in the UAE by decision-makers, particularly on industrial and vehicle pollution restrictions. The drawbacks of this work are that some datasets from

ground stations were incomplete. Additionally, the baseline was only a single year (i.e., 2019) due to the limited temporal scale of TROPOMI/Sentinel-5P data, and therefore the outcomes may change slightly when providing extra datasets. Further study is recommended to examine the correlation of air pollutants and SUHII with COVID-19 cases in the UAE.

CRediT authorship contribution statement

Abduldaem S. Alqasemi: Conceptualization, Methodology, Software, Validation, Formal analysis, Data curation, Writing- Original draft preparation and editing, Visualization, Investigation. **Mohamed E. Hereherb**: Conceptualization, Supervision, Writing- Reviewing and Editing. **Gordana Kaplan:** Conceptualization, Formal analysis, Software, Writing- Reviewing and Editing. **Ayad M. Fadhil Al-Quraishi**: Supervision, Writing- Reviewing and Editing. **Hakim Saibi**: Supervision, Writing- Reviewing and Editing. All authors have read and approved the final version of the manuscript for publication.

Declaration of competing interest

The authors declare that they have no known competing financial interests or personal relationships that could have appeared to influence the work reported in this paper.

Acknowledgements

The authors would like to thank the anonymous reviewers for their constructive comments on an earlier version of this paper. The authors are also grateful to the United Arab Emirates University for funding this work. We Thank the workers on the frontline against coronavirus.

References

Agarwal, A., Kaushik, A., Kumar, S., Mishra, R.K., 2020. Comparative study on air quality status in Indian and Chinese cities before and during the COVID-19 lockdown period. Air Qual. Atmos. Health 13, 1167–1178. https://doi.org/10.1007/s11869-020-00881-z.

Al Otaibi, M., Farahat, A., Tawabini, B., Omar, M.H., Ramadan, E., Abuelgasim, A., Singh, R.P., 2019. Long-term aerosol trends and variability over Central Saudi Arabia using optical characteristics from Solar Village AERONET measurements. Atmosphere 10, 752. https://doi.org/10.3390/atmos10120752.

Alahmad, B., Tomasso, L.P., Al-Hemoud, A., James, P., Koutrakis, P., 2020. Spatial distribution of land surface temperatures in Kuwait: Urban Heat and Cool Islands. Int. J. Environ. Res. Public Health 17, 1–11. https://doi.org/10.3390/ijerph17092993.

Alawadi, K., Khanal, A., Almulla, A., 2018. Land, urban form, and politics: a study on Dubai's housing landscape and rental affordability. Cities 81, 115–130. https://doi.org/10.1016/j.cities.2018.04.001.

Alghamdi, A.S., Moore, T.W., 2015. Detecting temporal changes in Riyadh's Urban Heat Island. Pap. Appl. Geogr. 1, 312–325. https://doi.org/10.1080/23754931.2015.1084525.

Alqasemi, A., Hereher, M., Al-Quraishi, A., Saibi, H., Aldahan, A., Abuelgasim, A., 2020. Retrieval of monthly maximum and minimum air temperature using MODIS Aqua land surface temperature data over the United Arab Emirates (UAE). Geocarto Int. https://doi.org/10.1080/10106049.2020.1837261.

Alseroury, F.A., 2015. The Effect of Pollutants on Land Surface Temperature Around Power Plant. pp. 17–21.

Archer, C.L., Cervone, G., Golbazi, M., Fahel, N. Al, Hultquist, C., 2020. Changes in Air Quality and Human Mobility in the U.S. During the COVID-19 Pandemic.

Baldasano, J.M., 2020. COVID-19 lockdown effects on air quality by NO2 in the cities of Barcelona and Madrid (Spain). Sci. Total Environ. 741, 140353. https://doi.org/10.1016/j.scitotenv.2020.140353.

Barbulescu, A., Nazzal, Y., 2020. Statistical analysis of dust storms in the United Arab Emirates. Atmos. Res. 231, 104669. a.alqasemi@uaeu.ac.ae https://doi.org/10.1016/j.atmosres.2019.104669.

Briz-Redón, Á., Serrano-Aroca, Á., 2020. The effect of climate on the spread of the COVID-19 pandemic: a review of findings, and statistical and modelling techniques. Prog. Phys. Geogr. Earth Environ. 44, 591–604. https://doi.org/10.1177/0309133320946302.

Bukhari, Q., Jameel, Y., 2020. Will coronavirus pandemic diminish by summer? SSRN Electron. J. https://doi.org/10.2139/ssrn.3556998.

Cheng, L., Tao, J., Valks, P., Yu, C., Liu, S., Wang, Y., Xiong, X., Wang, Z., Chen, L., 2019. NO2 retrieval from the environmental trace gases monitoring instrument (EMI): preliminary results and intercomparison with OMI and TROPOMI. Remote Sens. 11. https://doi.org/10.3390/rs11243017.

Clinton, N., Gong, P., 2013. MODIS detected surface urban heat islands and sinks: global locations and controls. Remote Sens. Environ. 134, 294–304. https://doi.org/10.1016/j.rse.2013.03.008.

Collivignarelli, M.C., Abbà, A., Bertanza, G., Pedrazzani, R., Ricciardi, P., Carnevale Miino, M., 2020. Lockdown for CoViD-2019 in Milan: what are the effects on air quality? Sci. Total Environ. 732, 139280. https://doi.org/10.1016/j.scitotenv.2020.139280.

Conticini, E., Frediani, B., Caro, D., 2020. Can atmospheric pollution be considered a co-factor in extremely high level of SARS-CoV-2 lethality in northern Italy? Environ. Pollut. 261, 114465. https://doi.org/10.1016/j.envpol.2020.114465.

Cui, Y.Y., De Foy, B., 2012. Seasonal variations of the urban heat island at the surface and the near-surface and reductions due to urban vegetation in Mexico City. J. Appl. Meteorol. Climatol. 51, 855–868. https://doi.org/10.1175/JAMC-D-11-0104.1.

Cui, Y., Xiao, X., Doughty, R.B., Qin, Y., Liu, S., Li, N., Zhao, G., Dong, J., 2019. The relationships between urban-rural temperature difference and vegetation in eight cities of the Great Plains. Front. Earth Sci. 13, 290–302. https://doi.org/10.1007/s11707-018-0729-5.

Dantas, G., Siciliano, B., França, B.B., da Silva, C.M., Arbilla, G., 2020. The impact of COVID-19 partial lockdown on the air quality of the city of Rio de Janeiro, Brazil. Sci. Total Environ. 729, 139085. https://doi.org/10.1016/j.scitotenv.2020.139085.

Fan, C., Li, Y., Guang, J., Li, Z., Elnashar, A., Allam, M., de Leeuw, G., 2020. The impact of the control measures during the COVID-19 outbreak on air pollution in China. Remote Sens. 12. https://doi.org/10.3390/rs12101613.

FAO, 2008. AQUASTAT Country Profile – United Arab Emirates. Food and Agriculture Organization of the United Nations (FAO), Rome.

Feizizadeh, B., Blaschke, T., 2013. Examining Urban Heat Island relations to land use and air pollution: multiple endmember spectral mixture analysis for thermal remote sensing. IEEE J. Selected Top. Appl. Earth Obs. Remote Sens. 6, 1749–1756. https://doi.org/10.1109/JSTARS.2013.2263425.

Filonchyk, M., Hurynovich, V., Yan, H., Gusev, A., Shpilevskaya, N., 2020. Impact assessment of COVID-19 on variations of SO2, NO2, CO and AOD over East China. Aerosol Air Qual. Res. 20, 1530–1540. https://doi.org/10.4209/aaqr.2020.05.0226.

Gautam, S., 2020. The influence of COVID-19 on air quality in India: a boon or inutile. Bull. Environ. Contam. Toxicol. 1.

Griffin, D., Zhao, X., McLinden, C.A., Boersma, F., Bourassa, A., Dammers, E., Degenstein, D., Eskes, H., Fehr, L., Fioletov, V., Hayden, K., Kharol, S.K., Li, S., Makar, P., Martin, R.V., Mihele, C., Mittermeier, R.L., Krotkov, N., Sneep, M., Lamsal, L.N., ter Linden, M., van Geffen, J., Veefkind, P., Wolde, M., 2019. High-resolution mapping of nitrogen dioxide with TROPOMI: first results and validation over the Canadian Oil Sands. Geophys. Res. Lett. 46, 1049–1060. https://doi.org/10.1029/2018GL081095.

Hashim, B.M., Sultan, M.A., 2010. Using remote sensing data and GIS to evaluate air pollution and their relationship with land cover and land use in Baghdad City. Iran. J. Earth Sci. 2, 20–24.

Hu, L., Brunsell, N.A., 2013. The impact of temporal aggregation of land surface temperature data for surface urban heat island (SUHI) monitoring. Remote Sens. Environ. 134, 162–174. https://doi.org/10.1016/j.rse.2013.02.022.

Hu, X., Zhao, Z., Zhang, L., Liu, Z., Li, S., Zhang, X., 2019. A high-temperature risk assessment model for maize based on MODIS LST. Sustainability (Switzerland) 11. https://doi.org/10.3390/su11236601.

Isaifan, R.J., 2020. The dramatic impact of Coronavirus outbreak on air quality: has it saved as much as it has killed so far? Glob. J. Environ. Sci. Manag. 6, 275–288. https://doi.org/10.22034/gjesm.2020.03.01.

Islam, M.S., Tusher, T.R., Roy, S., Rahman, M., 2020. Impacts of nationwide lockdown due to COVID-19 outbreak on air quality in Bangladesh: a spatiotemporal analysis. Air Qual. Atmos. Health https://doi.org/10.1007/s11869-020-00940-5.

Kahya, C., Bektas Balcik, F., Burak Oztaner, Y., Guney, B., 2016. Determining land surface temperature relations with land use-land cover and air pollution. EGU General Assembly Conference Abstracts, EGU General Assembly Conference Abstracts pp. EPSC2016-16489.

Kaplan, G., Avdan, Z., 2020. COVID-19: Spaceborne Nitrogen Dioxide Over Turkey. Eskişehir Techn. Univ. J. Sci. Technol. A Appl. Sci. Eng. https://doi.org/10.18038/estubtda.724450.

Karagulian, F., Temimi, M., Ghebreyesus, D., Weston, M., Kondapalli, N.K., Valappil, V.K., Aldababesh, A., Lyapustin, A., Chaouch, N., Al Hammadi, F., Al Abdooli, A., 2019. Analysis of a severe dust storm and its impact on air quality conditions using WRF-Chem modeling, satellite imagery, and ground observations. Air Qual. Atmos. Health 12, 453–470. https://doi.org/10.1007/s11869-019-00674-z.

Karuppasamy, M.B., Seshachalam, S., Natesan, U., Ayyamperumal, R., Karuppannan, S., Gopalakrishnan, G., Nazir, N., 2020. Air pollution improvement and mortality rate during COVID-19 pandemic in India: global intersectional study. Air Qual. Atmos. Health https://doi.org/10.1007/s11869-020-00892-w.

Keeratikasikorn, C., Bonafoni, S., 2018. Satellite images and Gaussian parameterization for an extensive analysis of urban heat islands in Thailand. Remote Sens. 10. https://doi.org/10.3390/rs10050665.

Kerimray, A., Baimatova, N., Ibragimova, O.P., Bukenov, B., Kenessov, B., Plotitsyn, P., Karaca, F., 2020. Assessing air quality changes in large cities during COVID-19 lockdowns: The impacts of traffic-free urban conditions in Almaty, Kazakhstan. Sci. Total Environ. 730, 139179. https://doi.org/10.1016/j.scitotenv.2020.139179.

Khuzestani, R.B., Schauer, J.J., Wei, Y., Zhang, L., Cai, T., Zhang, Yang, Zhang, Yuanxun, 2017. Quantification of the sources of long-range transport of PM2.5 pollution in the Ordos region, Inner Mongolia, China. Environ. Pollut. 229, 1019–1031. https://doi.org/10.1016/j.envpol.2017.07.093.

Lazzarini, M., Marpu, P.R., Ghedira, H., 2013. Temperature-land cover interactions: the inversion of urban heat island phenomenon in desert city areas. Remote Sens. Environ. 130, 136–152. https://doi.org/10.1016/j.rse.2012.11.007.

Li, Q., Guan, X., Wu, P., Wang, X., Zhou, L., Tong, Y., Ren, R., Leung, K.S.M., Lau, E.H.Y., Wong, J.Y., 2020a. Early transmission dynamics in Wuhan, China, of novel coronavirus–infected pneumonia. N. Engl. J. Med. 26 382 (13), 1199–1207.

Li, L., Li, Q., Huang, L., Wang, Q., Zhu, A., Xu, J., Liu, Ziyi, Li, H., Shi, L., Li, R., Azari, M., Wang, Y., Zhang, X., Liu, Zhiqiang, Zhu, Y., Zhang, K., Xue, S., Ooi, M.C.G., Zhang, D., Chan, A.,

2020b. Air quality changes during the COVID-19 lockdown over the Yangtze River Delta Region: an insight into the impact of human activity pattern changes on air pollution variation. Sci. Total Environ. 732, 139282. https://doi.org/10.1016/j.scitotenv.2020.139282.
Li, H., Xu, X.-L., Dai, D.-W., Huang, Z.-Y., Ma, Z., Guan, Y.-J., 2020c. Air pollution and temperature are associated with increased COVID-19 incidence: a time series study. Int. J. Infect. Dis. 97, 278–282. https://doi.org/10.1016/j.ijid.2020.05.076.
Lin, P., Gou, Z., Lau, S.S.Y., Qin, H., 2017. The impact of urban design descriptors on outdoor thermal environment: a literature review. Energies 10, 1–20. https://doi.org/10.3390/en10122151.
Lorente, A., Boersma, K.F., Eskes, H.J., Veefkind, J.P., van Geffen, J.H.G.M., de Zeeuw, M.B., Denier van der Gon, H.A.C., Beirle, S., Krol, M.C., 2019. Quantification of nitrogen oxides emissions from build-up of pollution over Paris with TROPOMI. Sci. Rep. 9, 20033. https://doi.org/10.1038/s41598-019-56428-5.
Lowe, S.A., 2016. An energy and mortality impact assessment of the urban heat island in the US. Environ. Impact Assess. Rev. 56, 139–144. https://doi.org/10.1016/j.eiar.2015.10.004.
Lu, N., Liang, S., Huang, G., Qin, J., Yao, L., Wang, D., Yang, K., 2018. Hierarchical Bayesian space-time estimation of monthly maximum and minimum surface air temperature. Remote Sens. Environ. 211, 48–58. https://doi.org/10.1016/j.rse.2018.04.006.
Lyapustin, A., Wang, Y., 2018. MCD19A2 MODIS/Terra+Aqua Land Aerosol Optical Depth Daily L2G Global 1km SIN Grid V006. NASA EOSDIS Land Processes DAAC https://doi.org/10.5067/MODIS/MCD19A2.006 (accessed 8.27.20).
Lyapustin, A., Wang, Y., Korkin, S., Huang, D., 2018. MODIS collection 6 MAIAC algorithm. Atmos. Meas. Tech. 11, 5741–5765. https://doi.org/10.5194/amt-11-5741-2018.
Mehdipour, V., Memarianfard, M., 2017. Application of support vector machine and gene expression programming on tropospheric ozone prognosticating for Tehran metropolitan. Civ. Eng. J. 3, 557–567.
Miles, V., Esau, I., 2017. Seasonal and spatial characteristics of Urban Heat Islands (UHIs) in northern West Siberian cities. Remote Sens. 9. https://doi.org/10.3390/rs9100989.
Moradi, M., Salahi, B., Masoodian, S.A., 2018. On the relationship between MODIS land surface temperature and topography in Iran. Physical Geography. Taylor & Francis https://doi.org/10.1080/02723646.2018.1426167.
Motesaddi, S., Hashempour, Y., Nowrouz, P., 2017. Characterizing of air pollution in Tehran: comparison of two air quality indices. Civ. Eng. J. 3, 749–758.
Mukherjee, S., Debnath, A., 2020. Correlation Between Land Surface Temperature and Urban Heat Island With COVID-19 in New Delhi, India. https://doi.org/10.21203/rs.3.rs-30416/v1.
Mulenga, D., Siziya, S., 2019. Indoor air pollution related respiratory ill health, a sequel of biomass use. SciMed. J. 1, 30–37.
Nakada, L.Y.K., Urban, R.C., 2020. COVID-19 pandemic: impacts on the air quality during the partial lockdown in São Paulo state, Brazil. Sci. Total Environ. 730, 139087. https://doi.org/10.1016/j.scitotenv.2020.139087.
Nemati, M., Ebrahimi, B., Nemati, F., 2020. Assessment of Iranian nurses' knowledge and anxiety toward COVID-19 during the current outbreak in Iran. Arch. Clin. Infect. Dis. 15.
Otmani, A., Benchrif, A., Tahri, M., Bounakhla, M., Chakir, E.M., El Bouch, M., Krombi, M., 2020. Impact of Covid-19 lockdown on PM10, SO2 and NO2 concentrations in Salé City (Morocco). Sci. Total Environ. 735, 139541. https://doi.org/10.1016/j.scitotenv.2020.139541.
Pathakoti, M., Muppalla, A., Hazra, S., Dangeti, M., Shekhar, R., Jella, S., Mullapudi, S.S., Andugulapati, P., Vijayasundaram, U., 2020. An assessment of the impact of a nation-wide lockdown on air pollution – a remote sensing perspective over India. Atmos. Chem. Phys. Discuss. 2020, 1–16. https://doi.org/10.5194/acp-2020-621.
Ranjan, A.K., Patra, A.K., Gorai, A.K., 2020a. Effect of lockdown due to SARS COVID-19 on aerosol optical depth (AOD) over urban and mining regions in India. Sci. Total Environ. 745, 141024. https://doi.org/10.1016/j.scitotenv.2020.141024.
Ranjan, A.K., Patra, A.K., Gorai, A.K., 2020b. Effect of lockdown due to SARS COVID-19 on aerosol optical depth (AOD) over urban and mining regions in India. Sci. Total Environ. 745, 141024. https://doi.org/10.1016/j.scitotenv.2020.141024.
Schwarz, N., Lautenbach, S., Seppelt, R., 2011. Exploring indicators for quantifying surface urban heat islands of European cities with MODIS land surface temperatures. Remote Sens. Environ. 115, 3175–3186. https://doi.org/10.1016/j.rse.2011.07.003.
Sekmoudi, I., Khomsi, K., Faieq, S., Idrissi, L., 2020. Covid-19 lockdown improves air quality in Morocco. arXiv preprint arXiv:2007.05417.
Sharma, S., Zhang, M., Anshika, Gao, J., Zhang, H., Kota, S.H., 2020. Effect of restricted emissions during COVID-19 on air quality in India. Sci. Total Environ. 728, 138878. https://doi.org/10.1016/j.scitotenv.2020.138878.
Tobías, A., Carnerero, C., Reche, C., Massagué, J., Via, M., Minguillón, M.C., Alastuey, A., Querol, X., 2020. Changes in air quality during the lockdown in Barcelona (Spain) one month into the SARS-CoV-2 epidemic. Sci. Total Environ. 726, 138540. https://doi.org/10.1016/j.scitotenv.2020.138540.
United Nations, 2019. World Urbanization Prospects: The 2018 Revision (ST/ESA/SER.A/420). Department of Economic and Social Affairs Population Division, New York.
Veefkind, J.P., Aben, I., McMullan, K., Förster, H., de Vries, J., Otter, G., Claas, J., Eskes, H.J., de Haan, J.F., Kleipool, Q., van Weele, M., Hasekamp, O., Hoogeveen, R., Landgraf, J., Snel, R., Tol, P., Ingmann, P., Voors, R., Kruizinga, B., Vink, R., Visser, H., Levelt, P.F., 2012. TROPOMI on the ESA Sentinel-5 precursor: a GMES mission for global observations of the atmospheric composition for climate, air quality and ozone layer applications. Remote Sens. Environ. 120, 70–83. https://doi.org/10.1016/j.rse.2011.09.027.
Venter, Z.S., Aunan, K., Chowdhury, S., Lelieveld, J., 2020. COVID-19 lockdowns cause global air pollution declines with implications for public health risk. medRxiv 2020.04.10.20060673 https://doi.org/10.1101/2020.04.10.20060673.
Wang, Q., Su, M., 2020. A preliminary assessment of the impact of COVID-19 on environment – a case study of China. Sci. Total Environ. 728, 138915. https://doi.org/10.1016/j.scitotenv.2020.138915.
Wei, J., Huang, W., Li, Z., Xue, W., Peng, Y., Sun, L., Cribb, M., 2019. Estimating 1-km-resolution PM2.5 concentrations across China using the space-time random forest approach. Remote Sens. Environ. 231, 111221. https://doi.org/10.1016/j.rse.2019.111221.
Weng, Q., Yang, S., 2006. Urban air pollution patterns, land use, and thermal landscape: an examination of the linkage using GIS. Environ. Monit. Assess. 117, 463–489. https://doi.org/10.1007/s10661-006-0888-9.
WHO, 2020a. WHO Coronavirus Disease (COVID-19) Dashboard [WWW Document]. URL. https://covid19.who.int/. (Accessed 13 September 2020).
WHO, 2020b. Coronavirus Disease 2019 (COVID-19) Situation Report – 51.
WHO, 2020c. Air pollution [WWW document]. URL. World Health Organizationhttps://www.who.int/health-topics/air-pollution#tab=tab_1%0AAir. (Accessed 24 July 2020).
Wu, X., Nethery, R.C., Sabath, B.M., Braun, D., Dominici, F., 2020. Exposure to air pollution and COVID-19 mortality in the United States: a nationwide cross-sectional study. medRxiv: the preprint server for health sciences 2020.04.05.20054502 https://doi.org/10.1101/2020.04.05.20054502.
Xu, K., Cui, K., Young, L.-H., Hsieh, Y.-K., Wang, Y.-F., Zhang, J., Wan, S., 2020. Impact of the COVID-19 event on air quality in Central China. Aerosol Air Qual. Res. 20, 915–929. https://doi.org/10.4209/aaqr.2020.04.0150.
Zhang, Z., Arshad, A., Zhang, C., Hussain, S., Li, W., 2020. Unprecedented temporary reduction in global air pollution associated with COVID-19 forced confinement: a continental and City scale analysis. Remote Sens. https://doi.org/10.3390/rs12152420.
Zhu, L., Huang, Q., Ren, Q., Yue, H., Jiao, C., He, C., 2020a. Identifying urban haze islands and extracting their spatial features. Ecol. Indic. 115, 106385. https://doi.org/10.1016/j.ecolind.2020.106385.
Zhu, Y., Xie, J., Huang, F., Cao, L., 2020b. Association between short-term exposure to air pollution and COVID-19 infection: evidence from China. Sci. Total Environ. 727, 138704. https://doi.org/10.1016/j.scitotenv.2020.138704.